Journal of Organometallic Chemistry 982 (2022) 122538

Contents lists available at ScienceDirect

Journal of Organometallic Chemistry

journal homepage: www.elsevier.com/locate/jorganchem

Alkyne Coupling and Cyclization on Metal Cluster Complexes. Additions and Couplings of Dimethyl acetylenedicarboxylate to $Ru_6(\mu_6\text{-}C)(CO)_{14}(\mu_3\text{-}\eta^4\text{-}C_4H_4)$

Richard D. Adams*, Meenal Kaushal, Mark D. Smith, Nutan D. Wakdikar

Department of Chemistry and Biochemistry, University of South Carolina, Columbia, SC 29208 USA

ARTICLE INFO

Article history:
Received 4 September 2022
Revised 14 October 2022
Accepted 15 October 2022
Available online 17 October 2022

Keywords:
Alkyne coupling
Aromatics
Ruthenium clusters
Diendiyl ligands
Alkyne complexes
Dimethylacetylenedicarboxylate

ABSTRACT

Reactions of the hexaruthenium cluster complex $Ru_6(\mu_6\text{-}C)(CO)_{14}(\mu_3{-}\eta^4{-}C_4H_4)$, 2 with dimethyl acetylenedicarboxylate (DMAD) at 25 °C yielded five new compounds: $Ru_6(\mu_5\text{-}C)(CO)_{16}(\mu{-}\eta^4{-}C_4H_4)$, 3; $Ru_6(\mu_6\text{-}C)(CO)_{14}[\eta^6\text{-}1,2\text{-}C_6H_4(CO_2Me)_2]$, 4; $Ru_6(\mu_5\text{-}C)(CO)_{14}(\mu{-}\eta^4{-}C_4H_4)[\mu_3{-}C_2(CO_2Me)_2]$, 5; $Ru_6(\mu_5\text{-}C)(CO)_{14}(\mu{-}\eta^4{-}C_4H_4)[\mu_3{-}C_2(CO_2Me)_2]$, 6 and $Ru_6(\mu_6\text{-}C)(CO)_{14}[\mu_3{-}\eta^6{-}1,2{-}C_6H_4(CO_2Me)_2]$, 7. Compounds 4 and 7 are isomers that contain the six-membered arene, dimethyl phthalate, $1,2{-}C_6H_4(CO_2Me)_2$, as a ligand. Compound 3 was formed as a side product in low yield (6%) by the simple addition of CO to 2. The addition of CO to 2 causes the cluster to open to that of a spiked, square pyramid. Direct reaction of CO to 2 provided 3 in a good yield (72%). A DMAD ligand was added to the cluster of 2 as a simple triply-bridging ligand to form open Ru_6 clusters in compounds 5 and 6. Addition of DMAD to 3 yielded the DMAD derivative $Ru_6(\mu_5\text{-}C)(CO)_{15}(\mu{-}\eta^4{-}C_4H_4)[\mu{-}C_2(CO_2Me)_2]$, 8 which contains a DMAD ligand bridging a basal edge of an opened spiked-square pyramidal Ru_6 cluster. Compound 5 was thermally converted to the new complex $Ru_6(\mu_5\text{-}C)(CO)_{14}[\mu_4{-}\eta^6{-}CHCHCHCC(CO_2Me)C(CO_2Me)](\mu\text{-}H)$, 9 that contains a bridging $CHCHCHCC(CO_2Me)C(CO_2Me)$ ligand formed by a coupling of the DMAD ligand to the bridging C_4H_4 ligand in 5 accompanied by a cleavage of one CH bond and formation of a bridging hydrido ligand. Decarbonylation of 3 with Me_3NO yielded the NMe_3 derivative $Ru_6(\mu_5\text{-}C)(CO)_{15}(\mu{-}\eta^4{-}C_4H_4)(NMe_3)$, 10 in which the NMe_3 ligand is coordinated to the spiked metal atom on the square-pyramidal Ru_5 cluster. Treatment of 4 and 7 with CO at 25 °C induced elimination of the $1,2{-}C_6H_4(CO_2Me)_2$ ligand to yield free dimethyl phthalate, 11 and formation of the known parent carbonyl complex $Ru_6(\mu_6\text{-}C)(CO)_{17}$. All of the new cluster compounds were characterized by single-crystal X-ray diffraction analyses.

1. Introduction

Compounds containing 6-membered aromatic rings have attracted the attention of chemists since the discovery of benzene in 1825 [1]. They are widespread in nature and are found in a variety of fragrances and flavorings and most importantly in a wide range of pharmaceuticals [2]. Aromatic compounds can be synthesized by a variety of methods [3–5]. Notably, the [2+2+2] cyclization of alkynes by using transition metal catalysts is known to yield a variety of aromatic compounds in all of their isomeric forms [5]. The metal-catalyzed coupling of alkynes occurs in a series of steps. To begin two alkynes are added to a metal complex and are then coupled to form a metallacycle. If only one metal atom is involved, then a metallacyclopentadienyl group, such as A, shown in Scheme 1, is typically formed [6]. If two or more metal atoms are involved, then diendiyl ligands will form and they usually adopt bridging coordinations by using the π-bonds between the carbon atoms to coordinate to the metal atoms, e. g. B [4a-b,6, 7] or C [8] see Scheme 1.

In recent studies, we have synthesized the zwitterionic hexaruthenium complex $Ru_6(\mu_6\text{-}C)(CO)_{14}[\mu_3\text{-}\eta^4\text{-}C_4H_4(NMe_3)]$, 1 that was transformed into the hexaruthenium carbonyl complex $Ru_6(\mu_6\text{-}C)(CO)_{14}(\mu_3{-}\eta^4\text{-}C_4H_4)$, 2 that contains the triply-bridging η^4 -butadiendiyl ligand C, R = H by elimination of NMe_3

* Corresponding author.
E-mail address: ADAMSRD@mailbox.sc.edu (R.D. Adams).

https://doi.org/10.1016/j.jorganchem.2022.122538
0022-328X/

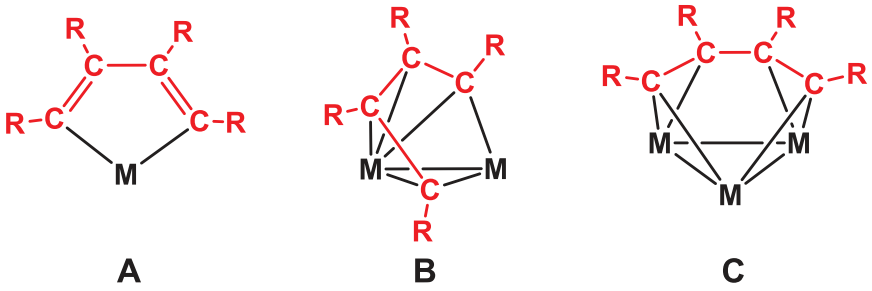

Scheme 1. Metallacycles formed by the coupling of alkynes to metal atoms.

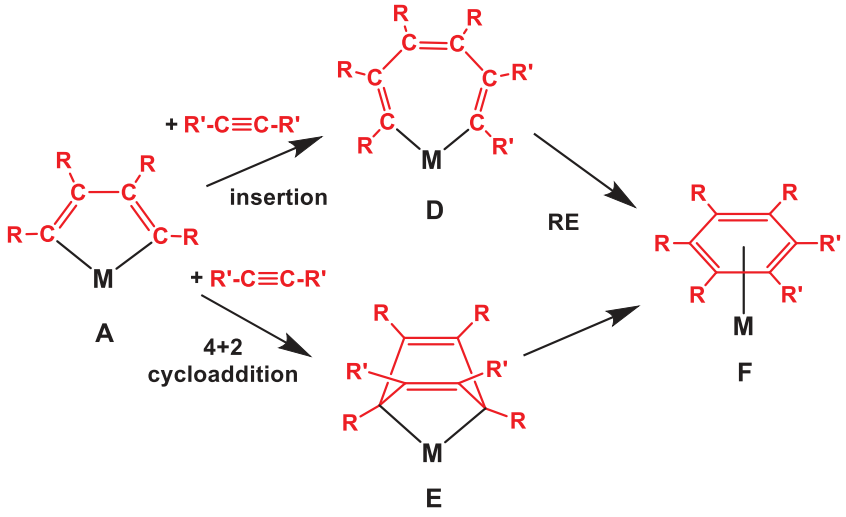

Scheme 2. Two mechanisms have been proposed for the cyclization of alkynes via the metallacyclopentadienyl ring system.

from the ammoniobutadienyl ligand, μ_3-η^4-CHCHCHCH$^+$NMe$_3$, in eq. (1) [8a].

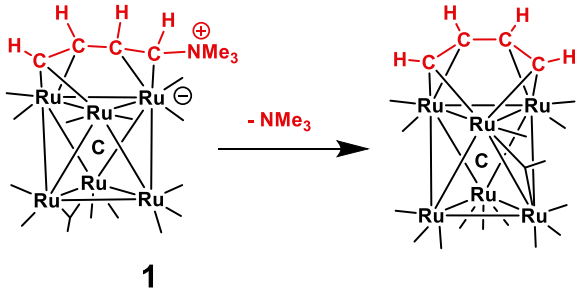

(1)

(1)

Mechanisms for the addition of a third alkyne to diendiyl ligands in the species A and B are still being actively investigated [9]. The two most widely discussed mechanisms are shown, in part, in Scheme 2. One involves insertion of a third alkyne into a metal – carbon bond of the diendiyl ligand, e. g. A, to yield a metallacycloheptatriene intermediate such as D that subsequently cyclizes by a C – C reductive-elimination to yield an arene ligand in a complex such as F and ultimately a free arene [9–10]. An alternative mechanism involves a 4 +2 cycloaddition to yield coordinated carbocyclic C_6 rings, such as E, that lead to an arene ligand and ultimately a free arene, Scheme 2. Support for the second mechanism has been increasing in recent years [9,10].

We have now investigated the reactions of 2 with the electron deficient alkyne, dimethyl acetylenedicarboxylate, $(MeO_2C)C{\equiv}C(CO_2Me)$, DMAD. The synthesis, structures and the chemistry of these new complexes which includes two complexes containing the coordinated arene dimethyl phthalate, 1,2-$C_6H_4(CO_2Me)_2$, are reported herein.

2. Experimental Section

2.1. General Data

All reactions were performed under an atmosphere of nitrogen. Reagent grade solvents were dried by the standard proce-

dures and were freshly distilled prior to use. Infrared spectra were recorded on a Thermo Scientific Nicolet IS10. ^{1}H NMR spectra were recorded on a Varian Mercury 300 spectrometer operating at 300.1 MHz. Mass spectral (MS) measurements performed by a direct-exposure probe by using electron impact ionization (EI) were made on a VG 70S instrument. Positive ion electrospray (ES+) mass spectral measurements were run on a Waters QTof API-US (quadrupole-TOF) spectrometer. $Ru_6(\mu_6\text{-}C)(CO)_{14}(\mu_3{-}\eta^4{-}C_4H_4)$, 2 was prepared according to the previously reported procedure [8a]. Dimethyl acetylenedicarboxylate (DMAD) and trimethylamine-N-oxide (Me_3NO) were purchased from Sigma-Aldrich and were used without further purification. Product separations were performed by TLC in the open air on Analtech 0.25 mm and 0.50 mm silica gel 60 Å F254 or alumina on glass plates.

2.2. Reaction of $Ru_6(\mu_6\text{-}C)(CO)_{14}(\mu_3\text{-}\eta^4\text{-}C_4H_4)$, 2 with DMAD

18.0 mg (0.017 mmol) of 2 was dissolved in 2.5 mL of dichloromethane-d_2 in an NMR tube. 6.0 μL of dimethyl acetylenedicarboxylate (DMAD) was added and the NMR tube was then sealed. The reaction mixture was kept at 25 °C for 3 days. After this period, resonances for the products were observed by ^{1}H NMR spectroscopy. Workup of the reaction mixture by TLC by using a hexane/methylene chloride solvent mixture yielded the following products in the order of elution: 1.2 mg (6.4% yield) of $Ru_6(\mu_5\text{-}C)(CO)_{16}(\mu\text{-}\eta^4\text{-}C_4H_4)$, 3, 1.0 mg (4.7% yield) of $Ru_6(\mu_6\text{-}C)(CO)_{14}[\eta^6\text{-}C_6H_4(CO_2Me)_2]$, 4, 1.0 mg (4.8% yield) of $Ru_6(\mu_5\text{-}C)(CO)_{14}(\mu\text{-}\eta^4\text{-}C_4H_4)[\mu_3\text{-}C_2(CO_2Me)_2]$, 5, 4.0 mg of (19.5% yield) of $Ru_6(\mu_5\text{-}C)(CO)_{14}(\mu\text{-}\eta^4\text{-}C_4H_4)[\mu_3\text{-}C_2(CO_2Me)_2]$, 6 and 8.0 mg (39% yield) of $Ru_6(\mu_6\text{-}C)(CO)_{14}[\mu_3\text{-}\eta^6\text{-}C_6H_4(CO_2Me)_2]$, 7. Spectral data for 3: IR, ν_{CO} (cm^{-1} in CH_2Cl_2): 2104.6 (w), 2081.4 (vs), 2049.5 (s), 2033.3 (vs), 2010.9 (m), 1968.0 (vw). ^{1}H NMR (in CD_2Cl_2, δ in ppm): 5.81 (m, br, CH), 5.65 (m, br, CH). Mass Spectrum (EI$^+$): M$^+$ - n(CO) 1119.5 – n(28), n = 0 - 16. Spectral data for 4: IR, ν_{CO} (cm^{-1} in CH_2Cl_2): 2080.2 (s), 2029.7 (vs), 1988.8 (m), 1828.5 (w, br). ^{1}H NMR (in CD_2Cl_2, δ in ppm): 6.03 (dd, CH, $^3J_{H3\text{-}H4}$ = 6.2 Hz), 5.69 (dd, CH, $^3J_{H3\text{-}H5}$ = 1.2 Hz), 3.83 (s, OCH_3). Mass Spectrum (EI$^+$): M$^+$ - n(CO) = 1205.0 – n(28), n = 1-14. Spectral data for 5: IR, ν_{CO} (cm^{-1} in CH_2Cl_2): 2094.4 (m), 2058.1 (vs), 2042.4 (s), 2032.5 (s), 1993.9 (w), 1927.4 (vw,br). ^{1}H NMR at 25 °C (δ in CD_2Cl_2) δ = 6.20 (m, 2H, CH) and 3.95 (s, $(OCH_3)_2$); at -90 °C (in CD_2Cl_2, δ): 7.32 (m, 1H, CH), 6.14 (m, 2H, CH), 3.94 (s, 3H, O(CH_3)), 3.87 (s, 3H, O(CH_3)) and 2.80 (m, 1H, CH). Mass Spectrum (ES$^+$): M$^+$ + Na$^+$ = 1228.0, M$^+$ -CO = 1174.0, M$^+$ -2 CO = 1146.0. Spectral data for 6: IR, ν_{CO} (cm^{-1} in CH_2Cl_2): 2094.0 (m), 2062.1 (vs), 2053.8 (vs, sh), 2038.8 (s), 2032.9 (s, sh), 2014.4 (w), 1978.2 (vw), 1938.0 (vw, br), 1892.3 (vw, br). ^{1}H NMR (in CD_2Cl_2, δ in ppm, 25 °C: 7.53 (br, 2H, CH), 6.94 (m, 2H, CH), 3.94 (s, 6H, OCH_3); at -90C): 8.58 (m, 1H, CH), 7.14 (m, 1H, CH), 6.85 (m, 1H, CH), 6.39 (m, 1H, CH), 3.95 (s, OCH_3), 3.78 (s, OCH_3). Mass Spectrum (EI$^+$): M$^+$ - n(CO) = 1205.0 – n(28), n = 0-14. Spectral data for 7: IR, ν_{CO} (cm^{-1} in CH_2Cl_2): 2085.3 (m), 2048.3 (s), 2034.1 (vs), 1981.3 (w), 1816.6 (vw,br). ^{1}H NMR (in CD_2Cl_2, δ in ppm): 4.63 (dd, CH, $^3J_{H3\text{-}H4}$ = 6.2 Hz), 4.41 (dd, CH, $^3J_{H3\text{-}H5}$ = 1.2 Hz), 3.76 (s, O(CH_3)). Mass Spectrum (EI$^+$): M$^+$ - n(CO) = 1205.0 – n(28), n = 1-14.

2.3. Reaction of 2 with CO

A 4.0 mg (0.0037 mmol) amount of 2 was dissolved in 2.5 mL of dichloromethane-d_2 in an NMR tube. CO gas was allowed to purge through this solution for 2 min and the NMR tube was then closed. The solution was then allowed to stand at room temperature for 24 h. After this period, the resonances for compound 3 were observed by ^{1}H NMR spectroscopy. Workup of the reaction mixture by TLC by using a hexane/methylene chloride solvent mixture yielded 3.0 mg (72% yield) of compound $Ru_6(\mu_5\text{-}C)(CO)_{16}(\mu\text{-}\eta^4\text{-}C_4H_4)$, 3.

2.4. Synthesis of 8 by Reaction of 3 with DMAD

A 5.0 mg (0.0045 mmol) amount of 3 was dissolved in 2.5 mL of toluene-d_8 in an NMR tube. To this, 3.0 μL of dimethyl acetylenedicarboxylate (DMAD) was added and the NMR tube was then closed. The reaction mixture was heated to 85 °C in a mineral oil bath for 48 h. After this period, the resonances for compound 8 were observed by ^{1}H NMR spectroscopy. Workup of the reaction mixture by TLC by using a hexane/methylene chloride solvent mixture yielded 2.0 mg (36% yield) of compound $Ru_6(\mu_5\text{-}C)(CO)_{15}(\mu\text{-}\eta^4\text{-}C_4H_4)[\mu\text{-}C_2(CO_2Me)_2]$, 8. Spectral data for 8: IR, ν_{CO} (cm^{-1} in CH_2Cl_2): 2103.8 (vw), 2084.5 (vs), 2058.1 (s), 2043.1 (m), 2026.2 (w), 2010.0 (w,sh), 1982.1 (vw), 1947.8 (vw), 1914.0 (vw). ^{1}H NMR (in CD_2Cl_2, δ in ppm): 5.95 (dd, 2H, CH, $^3J_{H1\text{-}H2}$ = 5.8 Hz), 5.60 (dd, 2H, CH, $^3J_{H1\text{-}H3}$ = 2.7 Hz), 3.82 (s, 6H, OCH_3). Mass Spectrum (ES$^+$): M+K$^+$+NCMe = 1311, M+K$^+$+NCMe-CO = 1283, M+K$^+$ = 1270, M+K$^+$-CO = 1242.

2.5. Thermal Transformation of 7

A 3.0 mg (0.0025 mmol) amount of 7 was dissolved in 2.5 mL of dichloromethane-d_2 in an NMR tube. This reaction mixture in this tube was then heated to 50 °C in a constant temperature mineral oil bath for 5 days. After this period, the resonances for compound 4 were observed by ^{1}H NMR spectroscopy. Workup of the reaction mixture by TLC by using a hexane/methylene chloride solvent mixture yielded 1.5 mg (50% conversion) of compound 4 and 0.3 mg of unreacted 7.

2.6. Thermal transformation of 5 to 9

A 2.0 mg amount of 5 was dissolved in 2.5 mL of dichloromethane-d_2 in a high-pressure NMR tube. The tube was sealed and the solution was heated at 65 °C for 4 days. The reaction was followed by NMR spectroscopy. Workup of the reaction was performed by TLC by using hexane/methylene chloride mixture to yield 0.5 mg of $Ru_6(\mu_5\text{-}C)(CO)_{14}[\mu_4{-}\eta^6{-}CHCHCHCC(CO_2Me)C(CO_2Me)](\mu\text{-}H)$, 9, 25% yield. Spectral Analysis of 9: IR, ν_{CO} (cm^{-1} in hexane): 2095.2(w), 2078.6(vs), 2055.7(s), 2046.7(s), 2032.1(w), 2020.3(m). ^{1}H NMR (in CD_2Cl_2, δ in ppm): 6.69 (m, CH, $^3J_{H\text{-}H}$ = 6.0 Hz, $^4J_{H\text{-}H}$ = 3.0 Hz), 5.94 (dd, CH, $^3J_{H\text{-}H}$ = 3.0 Hz, $^3J_{H\text{-}H}$ = 3.0 Hz), 5.71 (m, CH, $^3J_{H\text{-}H}$ = 6.3Hz, $^4J_{H\text{-}H}$ = 3.0 Hz), 3.95 (s, O(CH_3)$_3$), 3.87 (s, O(CH_3)$_3$), -21.9 (s, H). Mass Spectrum (EI$^+$): M$^+$ - nCO = 1205.0 – n(28), n = 0-14.

2.7. Synthesis of $Ru_6(\mu_5\text{-}C)(CO)_{15}(\mu{-}\eta^4{-}C_4H_4)(NMe_3)$, 10

A 9.0 mg (0.0084 mmol) amount of 3 was dissolved in 2.5 mL of toluene-d_8 in an NMR tube. To this solution 1.5 mg of Me_3NO was added and the mixture was then heated at 50 °C for 3 d. The reaction was monitored by ^{1}H NMR spectroscopy. Workup of the reaction mixture by TLC by using a hexane/methylene chloride solvent mixture yielded 1.0 mg (10.5% yield) of $Ru_6(\mu_5\text{-}C)(CO)_{15}(\mu{-}\eta^4{-}C_4H_4)(NMe_3)$, 10 and 1.0 mg of unreacted 3. Spectral Analyses of 10: IR, ν_{CO} (cm^{-1} in hexane): 2081.8(m), 2045.5(s), 2031.3(vs), 2009.3(w), 2001.4(w), 1982.1(vw), 1967.9(vw). ^{1}H NMR (in CD_2Cl_2, δ in ppm): 5.71 (dd, CH, $^3J_{H\text{-}H}$ = 3.9 Hz), 5.23 (dd, CH, $^3J_{H\text{-}H}$ = 3.9 Hz), 2.73 (s, N(CH_3)$_3$). Mass Spectrum (ESI$^+$): M$^+$ = 1150.0.

2.8. Isomerization of 6 to 5

A 1.0 mg amount of 6 was dissolved in 2.5 mL of dichloromethane-d_2 in an NMR tube. The solution was heated at

50 °C for 48 h. The reaction was monitored by ^{1}H NMR spectroscopy. Workup of the reaction mixture by TLC using a hexane/methylene chloride solvent mixture yielded 0.5 mg (50% yield) of 5. No 6 was recovered.

2.9. Reaction of 4 with CO

A 1.0 mg amount of 4 was dissolved in 2.5 mL of dichloromethane-d_2 in an NMR tube. CO gas was allowed to purge through this solution for 2 min and the NMR tube was then closed. The solution was then allowed to stand at room temperature for 24 h. After this period, new resonances attributed to dimethyl phthalate, 1,2-$C_6H_4(CO_2Me)_2$, 11 [11] were observed by ^{1}H NMR spectroscopy. Workup of the reaction mixture by TLC by using a hexane/methylene chloride solvent mixture yielded 0.4 mg of $Ru_6(\mu_6$-C)$(CO)_{17}$ and 0.1 mg of colorless band of 11 (62% yield) was obtained. Spectral Analyses for 11: ^{1}H NMR (in CD_2Cl_2, δ in ppm): 7.71 (m, CH), 7.56(m, CH), 3.87 (s, $O(CH_3)_3$). Mass Spectrum (EI^+): 194.0, M^+; 163.0, M^+ -OCH_3; 135.0, M^+ - CO_2CH_3; 104.0, M^+ - CO_2CH_3 + OCH_3.

2.10. Reaction of 7 with CO

A 7.0 mg amount of 7 was dissolved in 2.5 mL of dichloromethane-d_2 in an NMR tube. CO gas was allowed to purge through this solution for 2 min and the NMR tube was then closed. The solution was then allowed to stand at room temperature for 24 h. After this period, the resonances of the product 11 were observed by ^{1}H NMR spectroscopy. Workup of the reaction mixture by TLC by using a hexane/methylene chloride solvent mixture yielded 3.5 mg (55% yield) of $Ru_6(\mu_6$-C)$(CO)_{17}$ and 1.0 mg of a colorless band of 11 (88% yield).

2.11. Crystallographic Analyses

Single crystals of compounds 3 - 10 suitable for X-ray diffraction analyses were obtained by slow evaporation of solvent from solutions of the pure compounds at room temperature. X-ray intensity data were measured by using a Bruker D8 QUEST diffractometer equipped with a PHOTON-100 CMOS area detector and an Incoatec microfocus source (Mo K_α radiation, λ = 0.71073 Å) [12]. The raw area detector data frames were reduced, scaled, and corrected for absorption effects using the SAINT [12] and SADABS [13] programs. All structures were solved with SHELXT [14]. Subsequent difference Fourier calculations and full-matrix least-squares refinement against F^2 were performed by using SHELXL-2018 [14] or by using OLEX2 [15]. Full details for these analyses are available in the Supporting Information. Crystal data, data collection parameters, and results for each analysis are summarized in Table 1. Crystallographic data (cif files) for all of the structural analyses have also been deposited with the Cambridge Crystallographic Data Centre, CCDC 2204864-2204871 for compounds **3** - **10**, respectively.

3. Results

Reactions of the butadiendiylhexaruthenium cluster complex 2 with dimethyl acetylenedicarboxylate (DMAD) at 25 °C for 3 days yielded five new compounds, two of which contain the six-membered arene dimethyl phthalate, 1,2-$C_6H_4(CO_2Me)_2$, as a ligand. These compounds have been identified as $Ru_6(\mu_5$-C)$(CO)_{16}(\mu-\eta^4-C_4H_4)$, 3, (6.4% yield); $Ru_6(\mu_6$-C)$(CO)_{14}[\eta^6$-1,2-$C_6H_4(CO_2Me)_2]$, 4 (4.7% yield); $Ru_6(\mu_5$-C)$(CO)_{14}(\mu-\eta^4-C_4H_4)[\mu_3-C_2(CO_2Me)_2]$, 5, (4.8% yield); $Ru_6(\mu_5$-C)$(CO)_{14}(\mu-\eta^4-C_4H_4)[\mu_3-C_2(CO_2Me)_2]$, 6 (20% yield) and $Ru_6(\mu_6$-C)$(CO)_{14}[\mu_3-\eta^6-1,2-C_6H_4(CO_2Me)_2]$, 7 (39% yield).

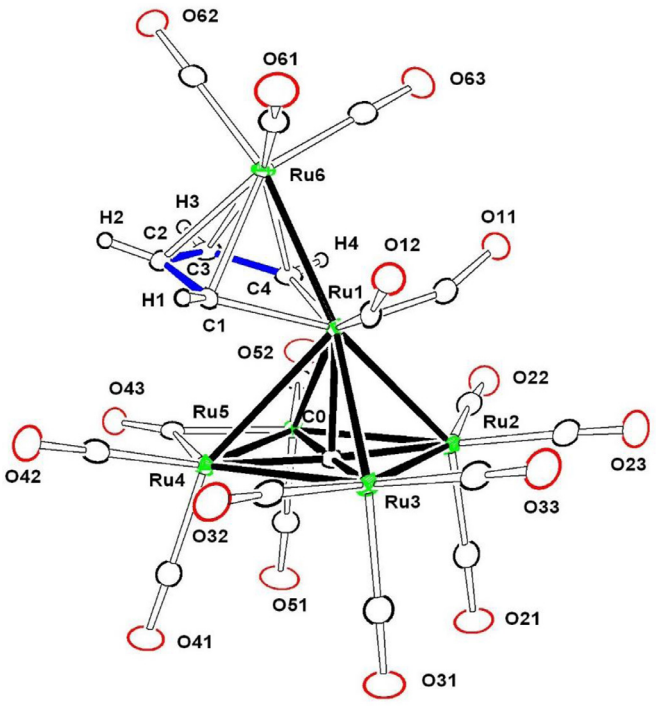

Figure 1. An ORTEP diagram of the molecular structure of the compound $Ru_6(\mu_5$-C)$(CO)_{16}(\mu-\eta^4-C_4H_4)$, 3 showing the 50% thermal ellipsoidal probability. Selected interatomic distances (Å) are as follows: Ru1-Ru2 2.80944(19), Ru1-Ru3 = 2.80862(19), Ru1-Ru4 = 2.96963(19), Ru1-Ru5 = 2.96241(19), Ru1-Ru6 = 2.74975(19), Ru2-Ru3 = 2.85374(19), Ru2-Ru5 = 2.9185(2), Ru3-Ru4 = 2.9228(2), Ru4-Ru5 = 2.75116(19), Ru1-C1 = 2.0897(16), Ru1-C4 = 2.0978(16), Ru6-C1 = 2.3026(15), Ru6-C2 = 2.1971(16), Ru6-C3 = 2.2053(16), Ru6-C4 = 2.3006(16), C1-C2 = 1.422(2), C2-C3 = 1.430(2), C3-C4 = 1.422(2).

All of the new compounds were characterized by IR, ^{1}H NMR, single-crystal X-ray diffraction analysis and mass spectrometry.

An ORTEP diagram of molecular structure of 3 is shown in Figure 1. Compound 3 contains a cluster of six ruthenium atoms that may be described as a 'spiked' square pyramid and appears to be the first example of such a structure in the literature. One of the ruthenium carbonyl groups, Ru(6), has been dislodged from the octahedral Ru_6 cluster as found in 2, but it remains attached to the apical ruthenium atom Ru(1) of the pentaruthenium carbide carbonyl cluster core by a Ru – Ru single bond. The Ru1-Ru6 distance, 2.74975(19) Å, is short, due in part to the presence of the bridging η^4-C_4H_4 butadiendiyl ligand, see below. The Ru – Ru distances in the square-pyramidal Ru_5 portion of the cluster, 2.80862(19) - 2.96963(19) Å, are similar to those in the related square-pyramidal Ru_5 cluster complexes, $Ru_5C(CO)_{15}$ and $Ru_5C(CO)_{14}PPh_3$ [16]. Compound 3 contains a total of sixteen carbonyl ligands distributed as shown in Figure 1. There is a bridging CO ligand across the Ru4 – Ru5 bond and semi-bridging CO ligands across the Ru1 – Ru2 and Ru1 – Ru3 metal – metal bonds. There is also a η^4-C_4H_4 butadiendiyl ligand that bridges the Ru1-Ru6 bond to the spiked-ruthenium atom Ru6 of the cluster. All four carbon atoms are π-bonded to Ru(6), Ru6-C1 = 2.3026(15) Å, Ru6-C2 = 2.1971(16) Å, Ru6-C3 = 2.2053(16) Å and Ru6-C4 = 2.3006(16) Å. The terminal carbon atoms C1 and C4 are also σ - bonded to the apical ruthenium atom of the square pyramid, Ru(1), Ru1-C1 = 2.0897(16) Å and Ru1-C4 = 2.0978(16) Å. The C – C bond distances within the butadiendiyl ligand are equal, C1–C2 = 1.422(2) Å, C2–C3 = 1.430(2) Å and C3–C4 = 1.422(2) Å within experimental error, indicating that the C – C bonding is fully delocalized across these four carbon atoms. ^{1}H NMR spectrum of 3 shows two broad deshielded resonances that can be assigned

Table 1
Crystal Data for the X-Ray Structural Analyses for Compounds 3 – 10.

Compound	3	4	5	6
Empirical formula	$C_{21}H_4O_{16}Ru_6$	$C_{25}H_{10}O_{18}Ru_6$	$C_{25}H_{10}O_{18}Ru_6$	$C_{25}H_{10}O_{18}Ru_6$
Formula weight	1118.66	1204.75	1204.75	1204.75
Crystal system	monoclinic	monoclinic	monoclinic	triclinic
Lattice parameters				
a (Å)	9.3269(3)	15.5552(8)	8.9118(3)	9.8368(7)
b (Å)	13.5819(5)	15.4822(8)	18.4294(6)	18.0052(13)
c (Å)	22.3396(8)	26.4000(17)	19.5202(7)	18.4116(13)
α (deg)	90.00	90.00	90.00	90.990(2)
β (deg)	98.315(2)	90.3845(19)	99.6110(10)	93.448(2)
γ (deg)	90.00	90.00	90.00	95.812(2)
V (Å^3)	2800.17(17)	6357.7(6)	3160.98(19)	3237.4(4)
Space group	$P2_1/c$	$I2/a$	$P2_1/c$	P-1
Z value	4	8	4	4
ρ_{calc} (g/cm^3)	2.654	2.517	2.532	2.472
μ (Mo Kα) (mm^{-1})	3.229	2.859	2.875	2.807
Temperature (K)	100(2)	301(2)	100(2)	300(2)
$2\theta_{max}$ (°)	65.31	55.198	60.078	50.22
No. Obs. (I>2σ(I))	10246	7328	9250	11480
No. of parameters	405	444	461	888
Goodness of fit (GOF)	1.080	1.017	1.119	1.105
Max. shift/error on final cycle	0.005	0.002	0.001	0.001
Residuals 2σ(I)[a]: R1; wR2	0.0193;0.0312	0.0323;0.0636	0.0192; 0.0384	0.0590; 0.1218
Absorption Corr,	multi-scan	multi-scan	multi-scan	multi-scan
Max/min	0.3605/ 0.2593	0.7456/0.6642	0.7460/0.6478	0.1770/ 0.1224
Largest peak in Final Diff. Map (e$^-$ / Å^3)	0.84	1.09	0.51	0.975
Compound	7	8	9	10
Empirical formula	$C_{25}H_{10}O_{18}Ru_6$	$C_{26}H_{10}O_{19}Ru_6$	$C_{27}H_{14.5}O_{18}Ru_6$	$C_{32}H_{22}NO_{15}Ru_6$
Formula weight	1204.75	1232.76	1233.31	1266.92
Crystal system	monoclinic	monoclinic	triclinic	triclinic
Lattice parameters				
a (Å)	14.7789(8)	15.3963(4)	12.020(2)	9.3716(3)
b (Å)	11.5156(7)	13.6012(4)	15.548(3)	14.9002(5)
c (Å)	18.4821(11)	16.9225(5)	19.912(4)	15.6455(5)
α (deg)	90.00	90.00	78.488(7)	107.8088(12)
β (deg)	98.3780(10)	111.385(2)	79.644(7)	102.7263(13)
γ (deg)	90.00	90.00	86.467(7)	102.6617(13)
V (Å^3)	3111.9(3)	2509.1(2)	3585.9(12)	1929.92(11)
Space group	$P2_1/c$	$P2_1/c$	P-1	P-1
Z value	4	4	4	2
ρ_{calc} (g/cm^3)	2.571	2.481	2.284	2.180
μ (Mo Kα) (mm^{-1})	2.920	2.759	2.537	2.355
Temperature (K)	100(2)	100(2)	300(2)	100(2)
$2\theta_{max}$ (°)	56.676	56.69	60.386	61.148
No. Obs. (I>2σ(I))	7757	8228	20958	11824
No. of parameters	457	478	921	586
Goodness of fit (GOF)	1.047	1.035	1.137	1.075
Max. shift/error on final cycle	0.001	0.001	0.002	0.002
Residuals 2σ(I)[a**]: R1; wR2	0.0231; 0.0410	0.0230; 0.0431	0.0321; 0.0644	0.0249;0.0400
Absorption Corr,	multi-scan	multi-scan	multi-scan	multi-scan
Max/min	0.3343/0.2810	0.6944/0.6059	0.2650/0.1971	0.5645/0.4605
Largest peak in Final Diff. Map (e$^-$ / Å^3)	0.65	0.77	0.854	0.548

[a] R1 = $\Sigma_{hkl}(||F_{obs}|-|F_{calc}||)/\Sigma_{hkl}|F_{obs}|$; wR2 = $[\Sigma_{hkl}w(|F_{obs}|-|F_{calc}|)^2/\Sigma_{hkl}wF^2{}_{obs}]^{1/2}$; $w = 1/\sigma^2(F_{obs})$; GOF = $[\Sigma_{hkl}w(|F_{obs}|-|F_{calc}|)^2/(n_{data} - n_{vari})]^{1/2}$

to the CH protons of the C_4H_4 ligand, δ = 5.81 (br, 2H) and 5.65 (br, 2H).

The bridging η^4–C_4H_4 ligand in 3 serves formally as a six-electron donor and with a total of sixteen CO ligands, compound 3 obtains a total of 90 cluster valence electrons which is in accord with both the effective atomic number rule (EAN) and the polyhedral skeletal electron pair (PSEP) counting method as applied to an apex-spiked, square pyramidal cluster of six transition metal atoms [17]. Compound 3 contains two more CO ligands than its precursor complex 2, and as expected, when compound 2 was exposed to an atmosphere of CO at room temperature for 24 h, compound 3 was obtained in a good yield (72%) simply by the addition of two equivalents of CO.

ORTEP diagrams of the molecular structures of 4 and 7 are shown in Figures 2 and 3, respectively. Compounds 4 and 7 are isomers that both contain an η^6-π-coordinated dimethyl phthalate, 1,2-$C_6H_4(CO_2Me)_2$, arene as a ligand. Both compounds contain an octahedral cluster of six ruthenium atoms with a carbido ligand in the center as found the parent compound 2. In 4 the 1,2-$C_6H_4(CO_2Me)_2$ ligand is coordinated in a terminal η^6-fashion to only one of the ruthenium atoms Ru(1) of the cluster while in 7, the 1,2-$C_6H_4(CO_2Me)_2$ ligand is coordinated in a triply-bridging, η^6-fashion to one of the triangular faces, Ru(1)-Ru(2)-Ru(3), of the Ru_6 cluster.

Interestingly, when a solution of 7 was heated at 50 °C for 5 days, it was converted into compound 4 in 50% yield. The reverse transformation does not occur which indicates that compound 7 is an intermediate and precursor to compound 4 in the series of reactions. Transformations of triply-bridging arene ligands into terminally-coordinated arene ligands in ruthenium cluster com-

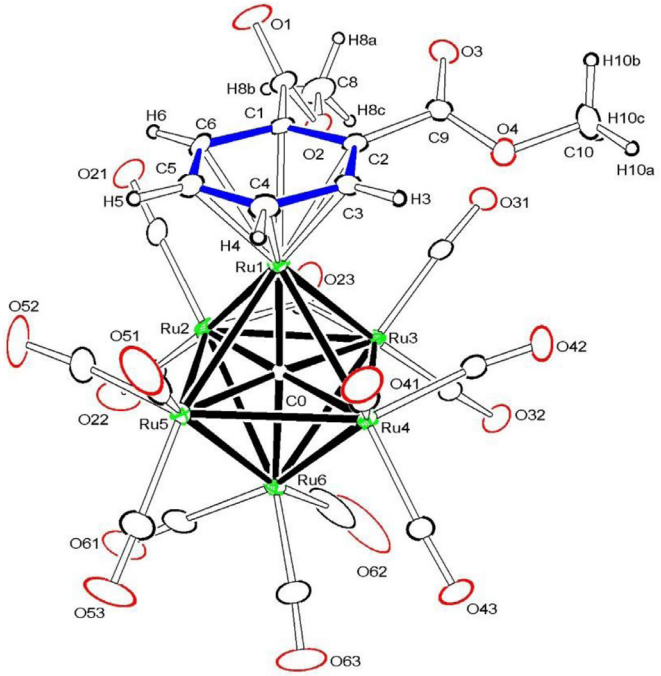

Figure 2. An ORTEP diagram of the molecular structure of the compound $Ru_6(\mu_6\text{-}C)(CO)_{14}[\eta^6\text{-}1,2\text{-}C_6H_4(CO_2Me)_2]$, 4 showing the 15% thermal ellipsoidal probability. Selected interatomic distances (Å) are as follows: Ru1-C1 = 2.257(4), Ru1-C2 = 2.279(5), Ru1-C3 = 2.242(5), Ru1-C4 = 2.221(5), Ru1-C5 = 2.236(5), Ru1-C6 = 2.253(4), C1-C2 = 1.422(7), C1-C6 = 1.415(7), C1-C7 = 1.510(7), C2-C3 = 1.406(7), C2-C9 = 1.508(7), C3-C4 = 1.402(7), C4-C5 = 1.401(8), C5-C6 = 1.393(7), O1-C7 = 1.194(6), O2-C7 = 1.312(6), O2-C8 = 1.445(6), O3-C9 = 1.199(6), O4-C9 =1.322(6), O4-C10 = 1.452(7).

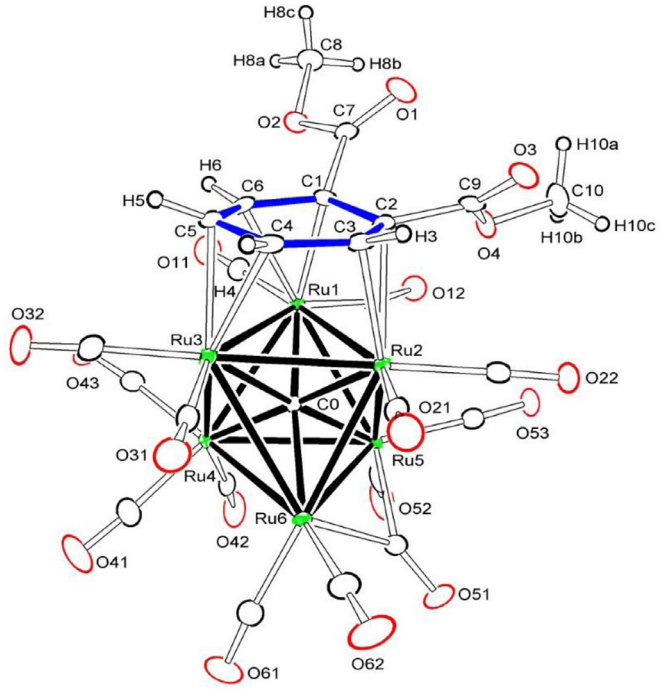

Figure 3. An ORTEP diagram of the molecular structure of the compound $Ru_6(\mu_6\text{-}C)(CO)_{14}[\mu_3\text{-}\eta^6\text{-}1,2\text{-}C_6H_4(CO_2Me)_2]$, 7, showing the 50% thermal ellipsoidal probability. Selected interatomic distances (Å) are as follow: Ru1-C1 = 2.140(3), Ru1-C6 = 2.327(3), Ru2-C2 = 2.365(3), Ru2-C3 = 2.194(3), Ru3-C4 = 2.364(3), Ru3-C5 = 2.217(3), C1-C2 = 1.471(4), C2-C3 = 1.423(4), C3-C4 = 1.451(4), C4-C5 = 1.399(4), C5-C6 = 1.439(4), C1-C6 = 1.438(4), C1-C7 = 1.501(4), C2-C9 = 1.504(4), O1-C7 = 1.202(4), O2-C7 = 1.340(4), O2-C8 = 1.453(3), O3-C9 = 1.205(4), O4-C9 = 1.337(4), O4-C10 = 1.443(4).

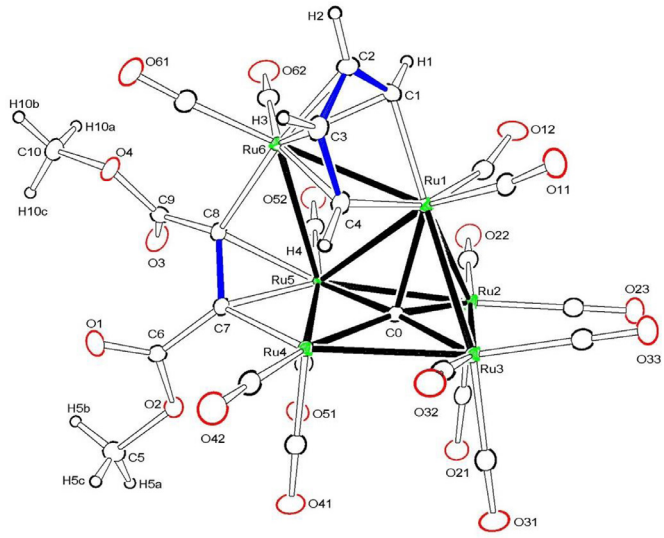

Figure 4. An ORTEP diagram of the molecular structure of the compound $Ru_6(\mu_5\text{-}C)(CO)_{14}(\mu\text{-}\eta^4\text{-}C_4H_4)[\mu_3\text{-}C_2(CO_2Me)_2]$, 5 showing the 40% thermal ellipsoidal probability. Selected interatomic distances (Å) are as follows: Ru1-Ru2 = 2.8100(2), Ru1-Ru3 = 2.8545(2), Ru1···Ru4 = 3.3627(2), Ru1-Ru5 = 3.0304(2), Ru1-Ru6 = 2.8643(2), Ru2-Ru3 = 2.8622(2), Ru2-Ru5 = 2.8784(2), Ru3-Ru4 = 2.9356(2), Ru4-Ru5 = 2.7074(2), Ru4···Ru6 = 3.750(1), Ru5-Ru6 = 3.0992(2), Ru1-C1 = 2.086(2), Ru1-C4 = 2.106(2), Ru6-C1 = 2.229(2), Ru6-C2 = 2.239(2), Ru6-C3 = 2.251(2), Ru6-C4 = 2.273(2), Ru6-C8 = 2.099(2), Ru5-C7 = 2.191(2), Ru5-C8 = 2.216(2), Ru4-C7 = 2.072(2), C1-C2 = 1.395(3), C2-C3 = 1.434(3), C3-C4 = 1.397(3), C6-C7 = 1.497(3), C7-C8 = 1.404(3), C8-C9 = 1.512(3), O1-C6 = 1.206(3), O2-C5 = 1.447(3), O2-C6 = 1.333(3), O3-C9 = 1.202(3), O4-C9 = 1.337(3), O4-C10 = 1.442(3).

plexes have been observed previously [18]. In both 4 and 7, the $C_6H_4(CO_2Me)_2$ ligand serves as a six-electron donor. Each cluster contains fourteen carbonyl ligands and thus both complexes contain a total of 86 cluster valence electrons and are in accord with the PSEP theory of electron counting for metal cluster complexes [17].

An ORTEP diagram of molecular structure of 5 is shown in Figure 4. Compound 5 contains six ruthenium atoms. The metal cluster of 5 can be described as an open square-pyramid of five Ru atoms. One of the apical-basal metal-metal bonds, Ru1···Ru4 at 3.3627(2) Å is missing. One of the edges of the Ru_5 pyramid, Ru1 –Ru5, contains the sixth ruthenium atom Ru6 as a bridge, Ru1-Ru6 = 2.8643(2) Å and Ru5-Ru6 = 3.0992(2) Å. There is a bridging η^4–C_4H_4 ligand across the Ru1-Ru6 bond. As in 3, it is π–bonded to Ru6, Ru6-C1 = 2.229(2) Å, Ru6-C2 = 2.239(2) Å, Ru6-C3 = 2.251(2) Å, Ru6-C4 = 2.273(2) Å and σ-bonded to Ru1, Ru1-C1 = 2.086(2) Å, Ru1-C4 = 2.106(2) Å. The C – C bond distances, C1-C2 = 1.395(3) Å and C3-C4 = 1.397(3) Å, are slightly shorter than the C2-C3 bond, 1.434(3) Å, and may contain more double character than the C2-C3 bond. There is a triply-bridging DMAD ligand having a di-σ + π coordination across the three ruthenium atoms, Ru4, Ru5 and Ru6, with Ru6-C8 = 2.099(2) Å, Ru5-C7 = 2.191(2) Å, Ru5-C8 = 2.216(2) Å, Ru4-C7 = 2.072(2) Å. There is no metal – metal bond between the atoms Ru4 and Ru6, Ru4···Ru6 = 3.750(1) Å.

The ^{1}H NMR spectrum of 5 varies with temperature in a way that is indicative of dynamical exchange activity. At 25 °C, the ^{1}H NMR spectrum exhibits only two resonances: one at δ = 6.20 (m, 2H) for two of the four C_4H_4 protons, and a singlet at δ = 3.95 (s, 6H) for the two OMe groups of the DMAD ligand, see Figure 5.

However, at -90 °C the ^{1}H NMR spectrum of 5 exhibits five resonances at δ = 7.32 (m, 1H, CH), 6.14 (m, 2H, CH), 3.94 (s, 3H, OCH_3), 3.87 (s, 3H, OCH_3) and 2.80 (m, 1H, CH). The OCH_3 resonances broaden as the temperature is raised and coalesce at -15

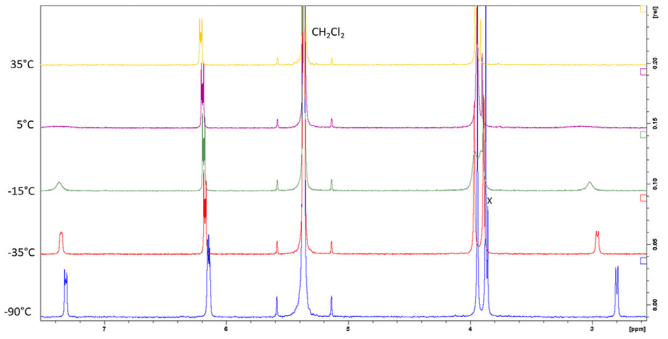

Figure 5. A stacked plot of the ^{1}H NMR spectra of 5 at different temperatures in CD_2Cl_2 solvent. The resonance labeled X is an impurity.

°C. The multiplets at 7.32 and 2.80 ppm broaden equally and reversibly, and collapse into the baseline at 25 °C, but because of the large shift difference between them, their averaged resonance was not observed even at temperatures moderately above 25 °C. It is apparent from these spectral changes that 5 is engaging in a dynamical exchange process that involves both the inequivalent methoxyl groups on the DMAD ligand and the inequivalent CH protons of the C_4H_4 ligand, although averaging of one pair of the CH protons, presumably the protons on the inner CH groups, C2 and C3, was still not slowed sufficiently to resolution even at -90 °C, presumably due to a much smaller shift difference between their resonances.

While there may be other mechanisms that can explain these observations, one that we find to be particularly attractive is shown in Scheme 3. In this process, compound 5 is reversibly exchanged with its enantiomer 5* via an intermediate such as I. In the process the inequivalent methoxy groups of the DMAD ligand are exchanged and the inequivalent alkenyl hydrogen atoms on C1 and C4, and C2 and C3 are exchanged in pairs, but those on C1 and C4 are not exchanged with those on C2 and C3, as observed. In the process the Ru(1) – Ru(5) and Ru6 – Ru5 metal – metal bonds in 5 are cleaved and new Ru – Ru bonds are formed to the symmetry equivalent of Ru4, which is Ru5 in the enantiomer 5*, see blue bonds in Scheme. Note: both enantiomers are present in the solid-state structure of the complex. The proposed intermediate I contains a mirror-like symmetry along the Ru1 – Ru6 bond.

With fourteen carbonyl ligands, a $\mu-\eta^4-C_4H_4$ ligand and one triply-bridging, DMAD ligand, compound 5 contains a total of 90 cluster valence electrons for the six metal atoms which is in accord with both the effective atomic number (EAN) rule and the PSEP theory for an edge-bridged, open, square-pyramidal cluster [17].

An ORTEP diagram of the molecular structure of 6 is shown in Figure 6. There are two structurally similar independent molecules of 6 in the asymmetric crystal unit. Compound 6 is an isomer of 5, and there are structural similarities between them. For example,

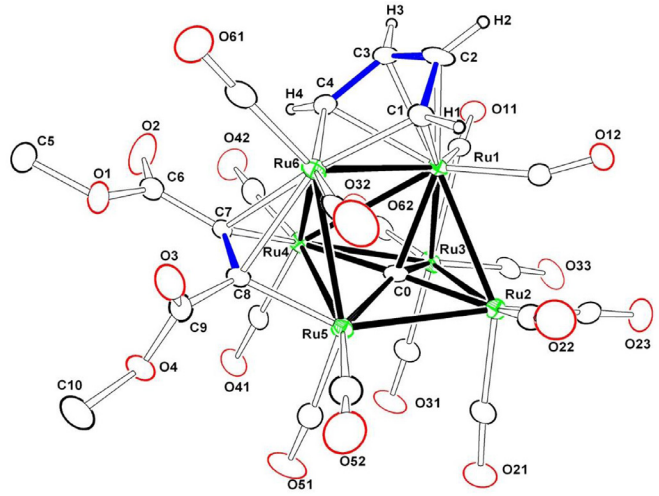

Figure 6. An ORTEP diagram of the molecular structure of the compound $Ru_6(\mu_5\text{-}C)(CO)_{14}(\mu-\eta^4-C_4H_4)[\mu_3-C_2(CO_2Me)_2]$, 6 showing the 15% thermal ellipsoidal probability. Selected interatomic distances (Å) for molecule A in the crystal are as follows: Ru1A-Ru2A = 2.8259(14), Ru1A-Ru3A = 2.8015(14), Ru1A-Ru4A = 3.0991(13), Ru1A···Ru5A = 3.604(1), Ru1A-Ru6A = 2.8523(14), Ru2A-Ru3A = 2.8472(15), Ru2A-Ru5A = 2.9314(14), Ru3A-Ru4A =2.8812(14), Ru4A-Ru5A = 2.8103(13), Ru4A-Ru6A = 3.0388(14), Ru5A-Ru6A = 2.8396(14), Ru1A···Ru5A = 3.604(4), Ru1A-C1A = 2.216(11), Ru1A-C2A = 2.237(12), Ru1A-C3A = 2.261(12), Ru1A- C4A = 2.377(12), Ru4A-C7A = 2.068(12), Ru5A-Ru6A = 2.8396(14), Ru5A-C8A = 2.044(12), Ru6A-C1A = 2.041(12), Ru6A-C4A = 2.095(12), Ru6A-C7A = 2.299(11), Ru6A-C8A = 2.270(11), C1A-C2A = 1.415(17), C2A-H2A = 0.9800, C2A-C3A = 1.411(19), C3A-C4A = 1.431(17), C6A-C7A = 1.483(17), C7A-C8A = 1.392(16), C8A-C9A = 1.496(16).

both compounds contain six ruthenium atoms, a bridging $\eta^4-C_4H_4$ ligand, a triply-bridging DMAD ligand and fourteen carbonyl ligands. However, the Ru_6 metal cluster of 6 has a slightly but significantly different structure from that of 5. The metal cluster in 6 could be described as a capped, square-pyramid, except that one of the apex to basal metal - metal bonds, namely Ru1 – Ru5 is missing, Ru1A···Ru5A = 3.604(1) Å, so the Ru_5 portion of the cluster has an open, square pyramidal shape.

Unlike 5, atom Ru6 in 6 is bonded to three other metal atoms instead of two, e. g. Ru1A-Ru6A = 2.8523(14) Å, Ru4A-Ru6A = 3.0388(14) Å, Ru5A-Ru6A = 2.8396(14) Å. In addition, although the $\eta^4-C_4H_4$ ligand in 6 bridges the metal – metal bond, Ru1 – Ru6, as it does in 5, in 6 it is $\pi-$bonded to Ru1 instead of Ru6, Ru1A-C1A = 2.216(11) Å, Ru1A-C2A = 2.237(12) Å, Ru1A-C3A = 2.261(12) Å, Ru1A- C4A = 2.377(12) Å and di-σ-bonded to Ru6, Ru6A-C1A = 2.041(12) Å, Ru6A-C4A = 2.095(12) Å. The C – C bond distances in the C_4H_4 ligand in 6 are equivalent within experimental error, C1A-C2A = 1.415(17) Å, C2A-C3A = 1.411(19) Å and C3A-C4A = 1.431(17) Å. The DMAD ligand in 6 is a triply-bridging ligand across the closed triangular Ru_3 group, Ru4, Ru5 and Ru6.

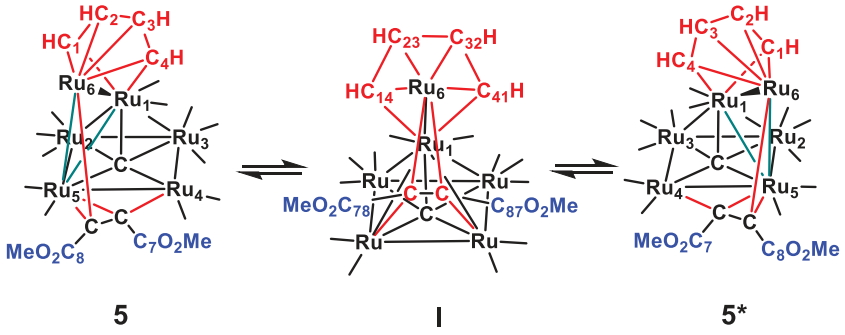

Scheme 3. A proposed mechanism for the dynamical exchange in 5.

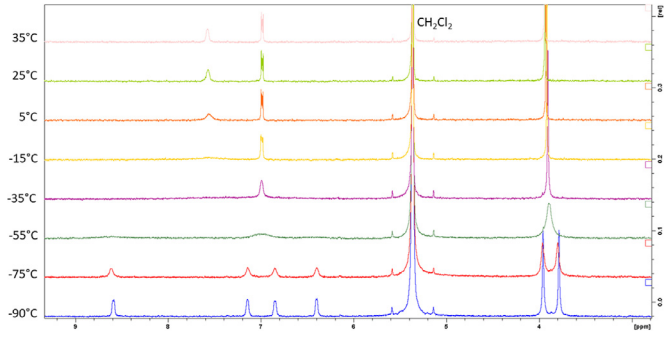

Figure 7. A stacked plot of the ^{1}H NMR spectra of 6 in CD_2Cl_2 at different temperatures.

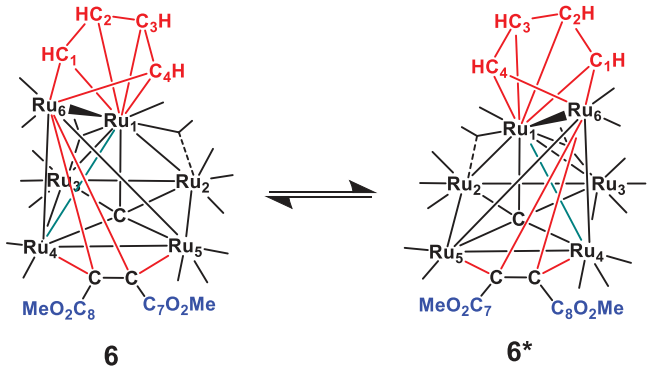

Scheme 4. A schematic of a proposed mechanism for the dynamical exchange process exhibited by compound 6.

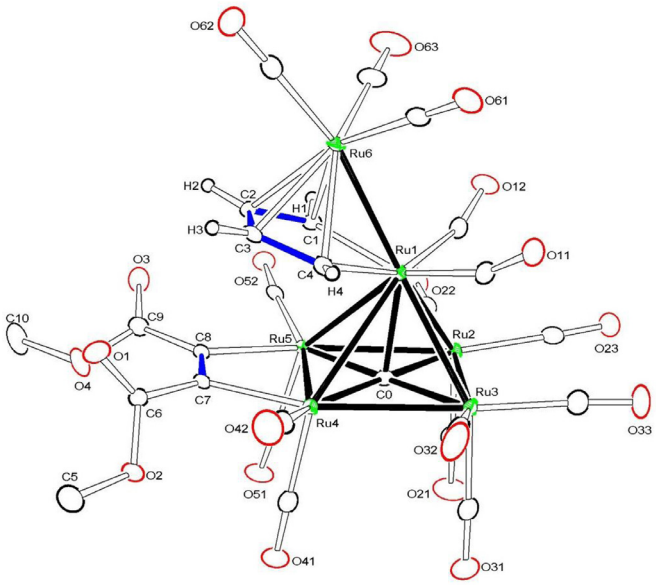

Figure 8. An ORTEP diagram of the molecular structure of the compound $Ru_6(\mu_5\text{-}C)(CO)_{15}(\mu-\eta^4-C_4H_4)[\mu-C_2(CO_2Me)_2]$, 8 showing the 40% thermal ellipsoidal probability. Selected interatomic distances (Å) are as follows: Ru1-Ru2 = 2.7925(3), Ru1-Ru3 = 2.8079(3), Ru1-Ru4 = 3.0092(3), Ru1-Ru5 = 2.9699(3), Ru1-Ru6 = 2.7436(3), Ru2-Ru3 = 2.8421(3), Ru2-Ru5 = 2.9243(3), Ru3-Ru4 = 2.8818(3), Ru4-Ru5 = 2.8080(3), Ru1-C1 = 2.097(3), Ru1-C4 = 2.102(3), Ru6-C1 = 2.291(3), Ru6-C2 = 2.206(3), Ru6-C3 = 2.216(3), Ru6-C4 = 2.294(3), Ru4-C7 = 2.091(3), Ru5-C8 = 2.095(3), C1-C2 = 1.426(4), C2-C3 = 1.426(4), C3-C4 = 1.410(4), C7-C8 = 1.320(4), C6-C7 = 1.471(4), C8-C9 = 1.479(4), O1-C6 = 1.200(3), O2-C5 = 1.439(4), O2-C6 = 1.342(3), O3-C9 = 1.201(3), O4-C9 = 1.340(4), O4-C10 = 1.449(4).

Compound 6 contains a total 90 cluster valence electrons and is in complete accord with the EAN Rule, i.e. an 18 electron configuration for each of the metal atoms.

The ^{1}H NMR spectra of 6 indicate that like 5, it is also dynamically active in solution, see Figure 7.

At -90 °C, the ^{1}H NMR of 6 in CD_2Cl_2 exhibits six resonances: four for the four inequivalent CH protons of the C_4H_4 ligand at δ = 8.58 (br, 1H), 7.14 (br, 1H), 6.85 (br, 1H), 6.39 (br, 1H) and two for the two inequivalent methyl groups of the DMAD ligand at δ =3.95 (s, 3H) and 3.78 (s, 3H). This spectrum is consistent with the structure as observed in the solid state. As the temperature is raised, all of the resonances begin to broaden and average in pairs: 7.14 ppm with 6.85 ppm, coalescence at ~ -65 °C; 8.58 ppm with 6.39 ppm, coalescence at -35 °C; and OCH_3 3.95 ppm with 3.78 ppm, coalescence at ~ -65 °C. At 25 °C the spectrum shows only three resonances for the averaged protons at 7.53 ppm (br, 2H, CH), 6.94 ppm (m, 2H, CH) and 3.94 ppm (s, 6H, OCH_3). The resonance averaging can be explained by the metal-shifting, dynamical exchange process shown in Scheme 4. In this simple process, the Ru1-Ru4 bond in 6 is reversibly cleaved and reformed between the atoms Ru1 and Ru5 to yield the enantiomer 6*, see blue bond. This bond to Ru(1) must move back and forth between atoms Ru(4) and Ru(5). The CH groups, C1 and C4, and C2 and C3 exchange in pairs as well as the methoxy groups on C7 and C8 on the DMAD ligands as observed experimentally.

Compounds 5 and 6 are isomers. When a sample of 6 was heated to 50 °C for 48 h, it was converted into compound 5 in 50 % yield.

When a sample of 3 was placed in an NMR tube with DMAD in toluene-d_8 solvent and was heated to 85 °C for 48 h, it eliminated one equivalent of CO, added one equivalent of DMAD and was converted to the new compound $Ru_6C(CO)_{15}(\mu-\eta^4-C_4H_4)[\mu-C_2(CO_2Me)_2]$, 8 in 36% yield. Compound 8 was also characterized structurally by a single-crystal X-ray diffraction analysis and an ORTEP diagram of its molecular structure is shown in Figure 8. Compound 8 contains a spiked, square-pyramidal cluster of six ruthenium atoms similar to that observed in 3. The Ru – Ru bonding in 8 is also very similar to that in 3. As in 3, the Ru1 – Ru6 bond to the "spike" is the shortest metal – metal bond in the cluster, Ru1-Ru6 = 2.7436(3) Å. The C_4H_4 ligand bridges the Ru1 – Ru6 bond as in 3 and may assist in the shortening of that bond. The C – C bonds within the C_4H_4 ligand are also very similar in length to those in 3, C1-C2 = 1.426(4) Å, C2-C3 = 1.426(4) Å, C3-C4 = 1.410(4) Å. There is a DMAD ligand bridging a basal edge of the square pyramidal cluster at the Ru4 – Ru5 bond in an unusual di-σ coordination fashion, Ru4-C7 = 2.091(3) Å and Ru5-C8 = 2.095(3) Å. It has replaced the bridging CO ligand in 3 and as a result the Ru4 –Ru5 bond increased in length by approx. 0.05 Å, Ru4-Ru5 = 2.8080(3) Å. The ^{1}H NMR spectrum for 8 shows three resonances: two for the two inequivalent pairs of C_4H_4 protons δ = 5.95 (dd, 2H, $^3J_{H1\text{-}H2}$ = 5.8 Hz, $^3J_{H1\text{-}H3}$ = 2.7 Hz) and 5.60 (dd, 2H, $^3J_{H1\text{-}H2}$ = 5.8 Hz, $^3J_{H\text{-}H}$ = 2.7 Hz) and one for the two equivalent methoxy groups on the DMAD ligand, δ = 3.82 (s, 6H, OCH_3). Compound 8 contains a total of 90 cluster valence electrons as found in 3 which is consistent with both the EAN and PSEP electron counting rules [17].

When a solution of compound 5 was heated to 65 °C for 4 days, it was converted the new compound $Ru_6C(CO)_{14}[\mu_4-\eta^6-CHCHCHCC(CO_2Me)C(CO_2Me)](\mu\text{-}H)$, 9 in 25% yield. Compound 9 was characterized by IR, ^{1}H NMR, single-crystal X-ray diffraction analysis and mass spectrometry. The crystal of 9 contains two independent molecules in the asymmetric unit. Both molecules are structurally similar. An ORTEP diagram of the molecular structure of molecule A in the crystal of 9 is shown in Figure 9.

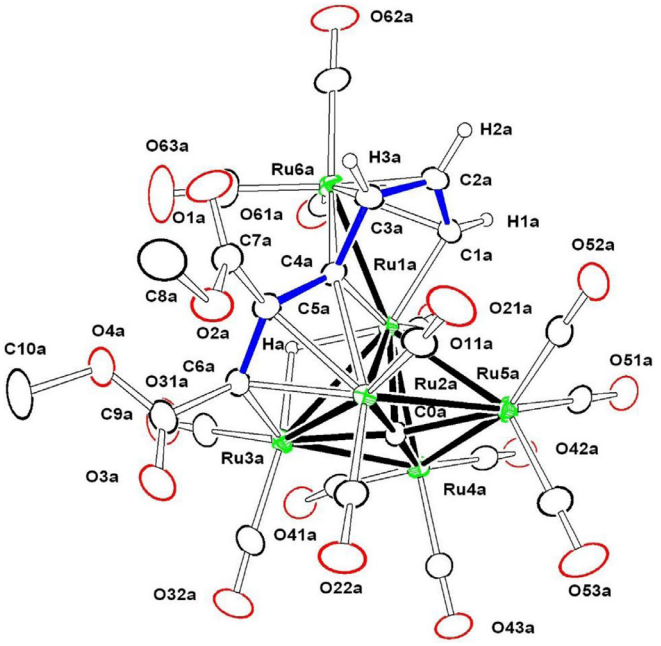

Figure 9. An ORTEP diagram of the molecular structure of the compound $Ru_6(\mu_5\text{-}C)(CO)_{14}[\mu_4\text{-}\eta^6\text{-}CHCHCHCC(CO_2Me)C(CO_2Me)](\mu\text{-}H)$, 9 showing the 20 % thermal ellipsoidal probability. Selected interatomic distances (Å) for molecule A are as follows: Ru1a-Ru6a = 2.7517(6), Ru1a-Ru2a = 2.8423(5), Ru1a-Ru3a = 2.8032(6), Ru1a-Ru4a = 2.8413(6), Ru1a-Ru5a = 2.7546(5), Ru2a-Ru3a = 2.7428(7), Ru2a-Ru5a = 2.8591(7), Ru3a-Ru4a = 2.9069(7), Ru4a-Ru5a = 2.8671(7), Ru1a-C1a = 2.053(4), Ru1a-C4a = 2.142(3), Ru2a-C4a = 2.309(3), Ru2a-C5a = 2.204(4), Ru2a-C6a = 2.209(4), Ru3a-C6a = 2.058(4), Ru4a-C0a = 1.971(3), Ru6a-C1a = 2.290(4), Ru6a-C2a = 2.234(4), Ru6a-C3a = 2.188(4), Ru6a-C4a = 2.332(3), C1a-C2a = 1.396(5), C2a-C3a = 1.413(5), C3a-C4a = 1.451(5), C4a-C5a = 1.454(5), C5a-C6a = 1.419(5), Ru1a-Ha = 1.87(3), Ru3a-Ha = 1.89(3).

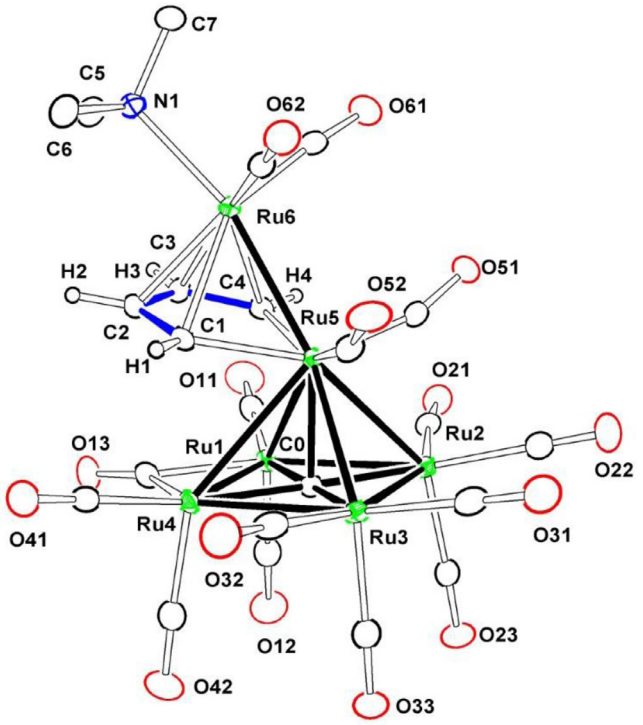

Figure 10. An ORTEP diagram of the molecular structure of the compound $Ru_6(\mu_5\text{-}C)(CO)_{15}(\mu\text{-}\eta^4\text{-}C_4H_4)(NMe_3)$, 10 showing the 50% thermal ellipsoidal probability. Selected interatomic distances (Å) are as follows: Ru5-Ru6 = 2.7422(3), Ru5-C1 = 2.119(2), Ru5-C4 = 2.093(2), Ru6-N1 = 2.2241(19), Ru6-C1 = 2.301(2), Ru6-C2 = 2.221(2), Ru6-C3 = 2.217(2), Ru6 -C4 = 2.282(2), N1-C5 = 1.487(3), N1-C6 = 1.489(3), N1-C7 = 1.489(3), C3-C4 = 1.417(3).

The cluster of 9 contains six ruthenium atoms in the arrangement of a spiked, square pyramid similar to those found in compounds 3 and 8. As in 3 and 8, the C_4-bridged Ru1 – Ru6 bond to the spike Ru6 is one of the shortest Ru – Ru bonds in the molecule, Ru1a-Ru6a = 2.7517(6) Å. The most interesting ligand in complex 9 is a quadruply-bridging η^6-1,2-C(CO_2Me)C(CO_2Me)CCHCHCH ligand that bridges the Ru1-Ru2-Ru3 triangular face of the Ru_5 square pyramid and extends to the metal spike Ru6. The six-carbon chain contains methylcarboxylate substituents on the two adjacent carbon atoms C5a and C6a at the one end and was evidently formed by the formation of a C – C bond to one of the carbon atoms of the DMAD ligand of 5 to one of the terminal CH groups of the C_4H_4 ligand of 5, C4a to C5a, C4a-C5a = 1.454(5) Å. The formation of the C – C bond was accompanied by a cleavage of the hydrogen atom from the carbon atom C4a. Atom C4a became a bridge across three of the metal atoms Ru1a, Ru2a and Ru6a, Ru1a-C4a = 2.142(3) Å, Ru2a-C4a = 2.309(3) Å, Ru6a-C4a = 2.332(3) Å, and the hydrogen atom was shifted to the cluster to become a bridging hydrido ligand Ha across the Ru1a and Ru3a bond. It was located and refined in the structural analysis. As expected, the resonance of the hydrido ligand appears at high field in the ^{1}H NMR spectrum at δ = -21.9. The three CH protons on the C_6-chain exhibit resonances at δ = 6.69 (m, $^3J_{H\text{-}H}$ = 6.0 Hz, $^4J_{H\text{-}H}$ = 3.0 Hz), 5.94 (dd, $^3J_{H\text{-}H}$ = 3.0 Hz, $^3J_{H\text{-}H}$ = 3.0 Hz) and 5.71 (m, $^3J_{H\text{-}H}$ = 6.3Hz, $^4J_{H\text{-}H}$ = 3.0 Hz) as expected and the methoxyl methyl groups appear as singlets at δ = 3.95 and 3.87. The bridging 1,2-C(CO_2Me)C(CO_2Me)CCHCHCH ligand serves as a 9-electron donor and the hydride as a one electron donor. With a total fourteen CO ligands, complex 9 achieves a total of 90 cluster valence electrons which is consistent with the observed spiked, square-pyramidal Ru_6 structure predicted by both the EAN rule and the PSEP theory of electron counting [17].

When compound 3 was allowed to react with Me_3NO in a toluene-d_8 solution at 50 °C for 3 d, it was converted to the new compound $Ru_6(\mu_6\text{-}C)(CO)_{15}(\mu\text{-}\eta^4\text{-}C_4H_4)(NMe_3)$, 10 in 10.5% yield. Compound 10 is a simple NMe_3 derivative of 3 formed by a Me_3NO-induced decarbonylation of 3 and the addition of the resultant NMe_3 to one of the metal atoms of the Ru_6 cluster. Compound 10 was characterized by a single-crystal, X-ray diffraction analysis and an ORTEP diagram of its molecular structure is shown in Figure 10.

As found in the parent complex 3, the metal cluster of 10 also contains a spiked, square-pyramidal Ru_6 structure. It contains a bridging η^4–C_4H_4 ligand across the Ru5 – Ru6 bond to the Ru6 spike. As expected, the bond distance Ru5-Ru6 = 2.7422(3) Å is slightly contracted due to the presence of the bridging C_4H_4 ligand. An NMe_3 ligand is located on the Ru6 spike *trans* to the Ru5 – Ru6 bond, Ru6-N1 = 2.2241(19) Å. The ^{1}H NMR spectrum of 10 exhibits two resonances for the two pairs of CH protons on the C_4H_4 ligand at δ = 5.71 (dd, $^3J_{H\text{-}H}$ = 3.9 Hz, $^3J_{H\text{-}H}$ = 3.9 Hz), 5.23 (dd, $^3J_{H\text{-}H}$ = 3.9 Hz, $^3J_{H\text{-}H}$ = 3.9 Hz) and one resonance δ = 2.73 for the methyl groups on NMe_3 ligand.

4. Discussion

Studies have shown that alkyne ligands readily undergo C-C bond coupling at mono- and dinuclear metal centers [5, 6, 19]. A number of metallacycles that have been formed by C – C coupling of two, three and four alkyne molecules at dinuclear metal centers have been structurally characterized [19]. Arenes are a common product in many of these coupling reactions and a variety of mechanisms have been proposed for their formation [5, 6, 9].

In this work, the reactions DMAD with the Ru_6 cluster complex 2 containing a triply-bridging C_4H_4 ligand have been in-

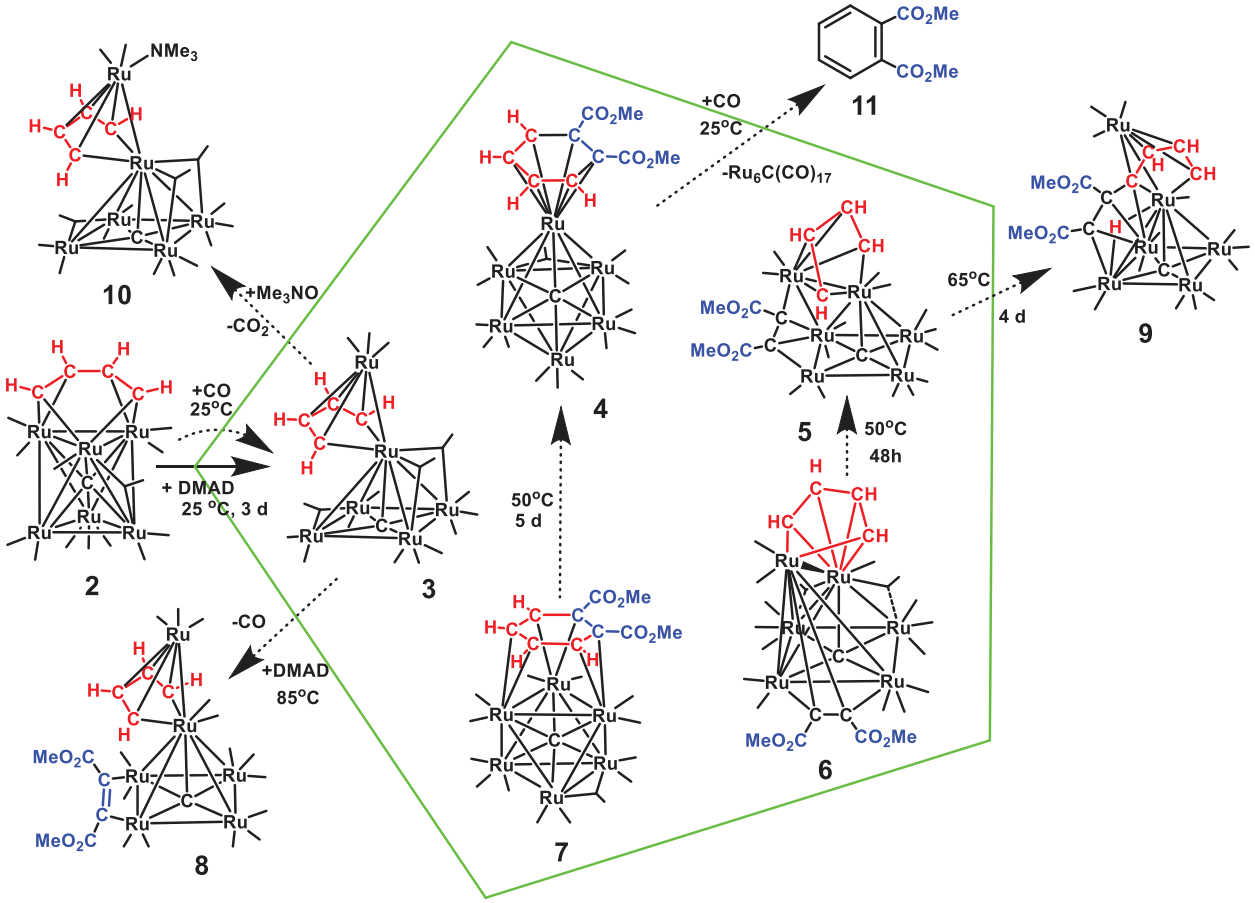

Scheme 5. A schematic summarizing the products and their relationships formed from the reactions of compound 2 with DMAD. The five initial products are shown within the green pentagon. CO ligands are shown only as lines from the Ru atoms.

vestigated. A summary of these reactions and products investigated in this study is shown in Scheme 5. Two isomeric arene-containing products, 4 and 7, were isolated that were found to contain an octahedral-shaped cluster of six ruthenium atoms with a π-coordinated dimethyl phthalate 1,2-$C_6H_4(CO_2Me)_2$ ligand that was formed by a cyclization coupling of the DMAD to the bridging C_4H_4 ligand. The mechanism of the formation of this arene ligand has not been determined, but it is notable that the arene ligand was observed only in complexes that contain an octahedral arrangement of the six ruthenium atoms. Also, the triply-bridging 1,2-$C_6H_4(CO_2Me)_2$ ligand in 7 was converted to a terminally, π-coordinated 1,2-$C_6H_4(CO_2Me)_2$ ligand in 4 simply by heating to 50 °C. When treated with CO, the 1,2-$C_6H_4(CO_2Me)_2$ ligand in 4 and 7 was displaced to yield the free arene 1,2-$C_6H_4(CO_2Me)_2$, 11 with formation of the parent carbonyl cluster complex $Ru_6(\mu_6\text{-}C)(CO)_{17}$ [20]. Compound 11 was also reportedly obtained by reaction of the rhodacyclopentadiene complex [(triphos)RhCl(η^2-C_4H_4)] (triphos = $MeC(CH_2PPh_2)_3$) with DMAD [6f].

Two additional products, 5 and 6, were also formed in the reaction of 2 with DMAD. In these products, a DMAD ligand is coordinated to metal atoms of the cluster as a bridging ligand. The increase in bonding electrons at the cluster caused by the addition of the DMAD, results in the cleavage of some of the metal – metal bonds in the metal cluster with transformation of it into edge-bridged, open-square-pyramidal species. Interestingly, when heated to 50 °C, compound 6 was converted to 5 by shifting the π–coordination of the bridging C_4H_4 ligand from the apex-metal atom Ru1 of the open square-pyramid to the edge-bridged metal atom Ru6 of the square pyramid of 5. When heated to 65 °C, compound 5 was converted to yet another isomer, 9, by formation of a carbon – carbon bond between the DMAD ligand and one of the terminal CH groups of the π-coordinated C_4H_4 ligand. In this process the CH bond of that CH group was cleaved and the hydrogen atom was converted to a bridging hydrido ligand on one of the Ru – Ru bonds of the metal cluster.

A minor coproduct 3 was obtained from the original reaction of 2 with DMAD, but it had nothing to do with the DMAD reagent. Compound 3 was a side product formed by the addition of two equivalents of CO only to 2. This was confirmed by an independent synthesis of 3 in a much better yield by the reaction of 2 with CO (1 atm) at 25 °C in the absence of DMAD. The CO in the original reaction was presumably scavenged from the reaction solution mixture to form 3 in a low yield. The increase in the number of CO ligands in the formation of 3 caused the Ru_6 cluster to open to yield the first example of a spiked, squared-pyramidal cluster of six ruthenium atoms. In an effort to obtain 5 or 6 from 3, a sample of 3 was treated directly with DMAD. Instead, the new compound 8 was formed by adding one equivalent of DMAD accompanied by the loss of one CO ligand. Compound 8 contains a DMAD bridging a basal edge of the square-pyramid of the spiked, squared-pyramidal cluster of metal atoms. Unfortunately, our efforts to obtain 5 or 6 by heating solutions of 8 were unsuccessful.

Finally, an effort was made to condense the metal cluster of 3 by decarbonylation by using Me_3NO. While decarbonylation did occur, cluster condensation did not. Instead, a molecule of NMe_3, produced by the reaction of the Me_3NO with a CO ligand on the cluster, was added to the metal atom spike Ru6, which was presumably the site of decarbonylation, to yield the compound 10, a NMe_3 derivative of 3.

5. Conclusions

Reactions of the octahedral Ru_6 cluster complex 2 containing a triply-bridging C_4H_4 ligand with the alkyne (DMAD) have yielded the cluster complexes 4 and 7 containing a dimethyl phthalate ligand formed by coupling of the DMAD to the C_4H_4 ligand. Competing reactions involving additions of the DMAD molecule to the metal atoms produced cluster-opened products 5 and 6.

The open cluster complex 3 containing a triply-bridging C_4H_4 ligand also formed a complex containing a DMAD ligand by substitution of a CO ligand. The open cluster complexes, 5 and 6, exhibit dynamical activities on the ^{1}H NMR timescale at 25 °C that are attributed to flexibility in the open metal clusters at this temperature. None of the open clusters containing DMAD ligands could be transformed into compounds 4 or 7 containing the dimethyl phthalate ligand, but when heated compound 5 was converted to the new compound 9 containing a C_6-chain by a coupling of the DMAD ligand to bridging C_4H_4 ligand. Unfortunately, it was also not possible to convert this C_6-chain of carbon atoms in 9 into a C_6 dimethyl phthalate ligand by further heating.

Appendix A. Supplementary Data

Experimental Details for the Syntheses; Crystallographic Analyses with Structure Solution and Refinement Details including Crystallographic Data (cif and checkcif files) and ORTEP structural diagrams and NMR spectra for all new new hexaruthenium compounds; Supplementary data related to this article can be found at http://dx.doi.org/10.1016/j.jorganchem.2022.122538 Crystallographic data (cif files) for all of the structural analyses have also been deposited with the Cambridge Crystallographic Data Centre, CCDC 2204864-2204871 for compounds 3 - 10, respectively. Copies of this information may be obtained free of charge from The Director, CCDC, 12 Union Road, Cambridge, CB2 1EZ UK [Fax. (int code) 44(1223)336-033, or Email: deposit@ccdc.cam.ac.uk or www: http://www.ccdc.cam.ac.uk.

Declaration of Competing Interest

The authors declare no competing financial interest.

Data Availability

Data will be made available on request.

Acknowledgement

This research was supported by grant 1764192 from the National Science Foundation. The Authors thank Dr. Perry Pellechia for assistance in recording the NMR spectra.

Supplementary materials

Supplementary material associated with this article can be found, in the online version, at doi:10.1016/j.jorganchem.2022.122538.

References

[1] D. Astruc, in Modern Arene Chemistry, D. Astruc, Ed., Wiley-VCH Pub., Weinheim, 2002.

[2] (a) A.G.A. Sá, C. de Meneses, P.H.H. de Araújo, D. de Oliveira, A review on enzymatic synthesis of aromatic esters used as flavor ingredients for food, cosmetics and pharmaceuticals industries, Trends Food Science & Tech 69 (2017) 95–105; (b) S.D. Roughley, A.M. Jordan, The Medicinal Chemist's Toolbox: An Analysis of Reactions Used in the Pursuit of Drug Candidates, J. Med. Chem. 54 (2011) 3451–3479.

[3] a) T. Li, T. Shikhara, J. Gascon, J. Ruiz-Martínez, Aromatics Production via Methanol-Mediated Transformation Routes, 2021 ACS Catal, 11 7780–7819; (b) A.M. Niziolek, O. Onel, C.A. Floudas, Production of benzene, toluene, and xylenes from natural gas via methanol: Process synthesis and global optimization, 2016 AIChE J, 62 1531–1556; (c) B.H. Davis, Alkane dehydrocyclization mechanism, 1999 Catal. Today, 53 443–516; d) P.G. Menon, P. Paál, Some Aspects of the Mechanisms of Catalytic Reforming Reactions, 1997 Ind. Eng. Chem. Res., 36 3282–3291; e) H. Heineman, G.A. Mills, J.B. Hattman, F.W. Kirsch, Houdriforming Reactions. Studies with Pure Hydrocarbons, 1953 Ind. Eng. Chem., 45 130–134; f) G.J. Anto, A.M. Aitani, J.M. Parera (Eds.), See *Catalytic Naphtha Reforming*, Eds., Marcel Dekkar Inc., New York, 1995.

[4] [a] A. Link, C. Sparr, Stereoselective arene formation, Chem. Soc. Rev. 47 (2018) 3804–3815; [b] H. Ito, Y. Segawa, K. Murakami, K. Itami, Polycyclic Arene Synthesis by Annulative π–Extension, J. Am. Chem. Soc. 141 (2019) 3–10.

[5] a) A. Roglans, A. Pla-Quintana, M. Solà, Mechanistic Studies of Transition-Metal-Catalyzed [2 + 2 + 2] Cycloaddition Reactions, Chem. Rev. 121 (2021) 1894–1979; b) P. Matton, S. Huvelle, M. Haddad, P. Phansavath, V. Ratovelomanana-Vidal, Recent Progress in Metal-Catalyzed [2+2+2] Cycloaddition Reactions, Synthesis 54 (2022) 4–32; c) S. Ohta, N. Miura, K. Saitoh, K. Itoh, S. Satoh, R. Miyamoto, M. Okazaki, Synthesis and Structures of Bis(indolyl)-Coordinated Titanium Dichlorido Complexes and Their Catalytic Application in the Cyclotrimerization of Alkynes, Organometallics 40 (2021) 2826–2835; d) L. Xu, S. Li, L. Jiang, T. Dong, G. Zhang, W. Zhang, Z. Gao, Revisiting reactions of alkynes with $Ru_3(CO)_{12}$: Effects of alkyne substituents and solvents on the structures of ruthenium cluster products, Inorg. Chim. Acta 485 (2019) 20–25; (e) J.A. Varela, C. Saá, CpRuCl- and CpCo-Catalyzed or Mediated Cyclotrimerizations of Alkynes and [2 + 2 + 2] Cycloadditions of Alkynes to Alkenes: A Comparative DFT Study, J. Organomet. Chem. 694 (2009) 143–149; (f) S. Saito, Y. Yamamoto, Recent Advances in the Transition-Metal-Catalyzed Regioselective Approaches to Polysubstituted Benzene Derivatives, Chem. Rev. 100 (2000) 2901–2915; (g) V. Gandon, C. Aubert, M. Malacria, Recent Progress in Co-Mediated [2 + 2 + 2] Cycloaddition Reactions, Chem. Commun. (2006) 2209–2217; (h) B.R. Galan, T. Rovis, Beyond Reppe, Building Substituted Arenes by [2 + 2 + 2] Cycloadditions of Alkynes, Angew. Chem., Int. Ed. 48 (2009) 2830–2834; (i) G. Domínguez, J. Pérez-Castells, Recent Advances in [2 + 2 + 2] Cycloaddition Reactions, Chem. Soc. Rev. 40 (2011) 3430–3444; (j) N. Weding, M. Hapke, Preparation and Synthetic Applications of Alkene Complexes of Group 9 Transition Metals in [2 + 2 + 2] Cycloaddition Reactions, Chem. Soc. Rev. 40 (2011) 4525–4538; (k) Y. Shibata, K. Tanaka, Rhodium-Catalyzed [2 + 2 + 2] Cycloaddition of Alkynes for the Synthesis of Substituted Benzenes: Catalysts, Reaction Scope, and Synthetic Applications, Synthesis 44 (2012) 323–350; (l) D.L.J. Broere, E. Ruijter, Recent Advances in Transition-Metal-Catalyzed [2+2+2]-Cyclo(co)trimerization Reactions, Synthesis 44 (2012) 2639–2672; (m) T. Shibata, K. Tsuchikama, Recent advances in enantioselective [2 + 2 + 2] cycloaddition, Org. Biomol. Chem. 6 (2008) 1317–1323; (n) Y. Yamamoto, T. Arakawa, R. Ogawa, K. Itoh, Ruthenium(II)-Catalyzed Selective Intramolecular [2 + 2 + 2] Alkyne Cyclotrimerizations, J. Am. Chem. Soc. 125 (2003) 12143–12160.

[6] (a) H. Yamazaki, Y. Wakatsuki, Cobalt Metallocycles XIII. Preparation and X-ray Crystallography of Cobaltacyclopentadiene and Dinuclear Cobalt Complexes, J. Organomet. Chem. 272 (1984) 251–263; (b) Y. Wakatsuki, O. Nomura, K. Kitaura, K Morokuma, H. Yamazaki, Cobalt Metallacycles, 11. On the Transformation of Bis(acetylene)cobalt to Cobaltacyclopentadiene, J. Am. Chem. Soc. 105 (1983) 1907–1912; (c) H. Yamazaki, Y. Wakatsuki, Cobalt Metallocycles I. One-Step and Stepwise Synthesis of Cobaltacyclopentadiene Complexes from Acetylenes, J. Organomet. Chem. 139 (1977) 157–167; (d) R.G. Gastinger, M.D. Rausch, D.A. Sullivan, G.J. Palenik, Synthesis and Molecular Structure of 1-(π-Cyclopentadienyl)-1-triphenylphosphine-2,3,4,5-tetrakis(pentafluorophenyl)cobaltole, J Am. Chem. Soc. 98 (1976) 719–723; (e) D.R. McALister, J.E. Bercaw, R.G. Bergman, Parallel reaction pathways in the cobalt-catalyzed cyclotrimerization of acetylenes, J. Am. Chem. Soc. 99 (1977) 1666–1668; (f) C. Bianchini, A. Meli, M. Peruzzini, A. Vacca, F. Vizza, Coupling of Two Ethyne Molecules at Rhodium versus Coupling of Two Rhodium Atoms at Ethyne. 2. Implications for the Reactivity. Catalytic and Stoichiometric Functionalization Reactions of Ethyne, Organometallics 10 (1991) 645–651.

[7] (a) E. Sappa, Complexes of transition metal carbonyls with alkynes. Closo- and nido-pentagonal bipyramidal clusters, J. Organomet. Chem. 573 (1977) 139–155; (b) G. Dettlaf, E. Weiss, Kristallstruktur, ^{1}H-NMR- und massenspektrum von tricarbonylferracyclopentadienetricarbonyleisen, $C_4H_4Fe_2(CO)_6$, J. Organomet. Chem 108 (1976) 213–223; (c) L. Xu, S. Li, L. Jiang, T. Dong, G. Zhang, W. Zhang, Z. Gao, Revisiting reactions of alkynes with $Ru_3(CO)_{12}$: Effects of alkyne substituents and solvents on the structures of ruthenium cluster products, Inorg. Chim. Acta 485 (2019) 20–25; (d) M. H. Chisholm, K. Folting, D. M. Hoffman, J. C. Huffman, J. Leonelli, The remarkable role of steric factors in the reactions of alkynes (HC≡CH and MeC≡CMe)with ditungsten hexa-alkoxides: crystal and molecular structures of W2(OPri)6(py)2(μ-C2H2), W2(OCH2But)6(py)2(μ-C2Me2), and W2(OPri)2(μ-C4R4)(C2R2), where R = H and Me (py = pyridine), *J. Chem. Soc., Chem. Commun.* (1983) 589-591.; [e] H. Omori, H. Suzuki, Y. Morooka, Preparation and structure determination of a dinuclear ruthenacyclopentadiene complex. Coupling of coordinated vinyl ligands, Organometallics 8 (1989) 1576–1578.

[8] (a) R.D. Adams, M.D. Smith, N.D. Wakdikar, Zwitterionic Ammoniumalkenyl Ligands in Metal Cluster Complexes. Synthesis, Structures and Transformations of Zwitterionic Trimethylammoniumalkenyl Ligands in Hexaruthenium Carbido Carbonyl Complexes, Inorg. Chem. 59 (2020) 1513–1521; (b) A.J. Blake, J.L. Haggitt, B.F.G. Johnson, S. Parsons, Alkyne based derivatives of $[Ru_6C(CO)_{17}]$ and the stepwise synthesis of $[Ru_6C(CO)_{13}(\eta^5\text{-}C_5H_5Ph_2)(\mu_3\text{-}CPh)]$, J. Chem. Soc., Dalton Trans (1997) 991–994; (c) A.A. Koridze, N.M. Astakhova, F.M. Dolgushin, A.I. Yanovsky, Y.T. Struchkov, P.V. Petrovskii, A Triosmium Cluster with a Novel

Mode of Metallacyclopentadiene Fragment Bonding. X-ray Structure and Reactivity of Os_3 (μ_3-η^1:η^1:η^2-C($SiMe_3$)C(Me)C(H)C(Ph)}($CO)_9$, Organometallics 14 (1995) 2167–2169.

[9] (a) J.H. Hardesty, J.B. Koerner, T.A. Albright, G.Y. Lee, Theoretical Study of the Acetylene Trimerization with CpCo, J. Am. Chem. Soc. 121 (1999) 6055–6067; (b) N. Agenet, V. Gandon, K.P.C. Vollhardt, M. Malacria, C. Aubert, Cobalt–Catalyzed Cyclotrimerization of Alkynes: The Answer to the Puzzle of Parallel Reaction Pathways, J. Am. Chem. Soc. 129 (2007) 8860–8871; (c) M. Martinez, M. del Carmen Michelini, I. Rivalta, N. Russo, E. Sicilia, Acetylene Cyclotrimerization by Early Second-Row Transition Metals in the Gas Phase. A Theoretical Study, Inorg. Chem. 44 (2005) 9807–9816; (d) D.-H. Kwon, M. Proctor, S. Mendoza, C. Uyeda, D.H. Ess, Catalytic Dinuclear Nickel Spin Crossover Mechanism and Selectivity for Alkyne Cyclotrimerization, ACS Catal 7 (2017) 4796–4804; (e) F. Calderazzo, G. Pampaloni, P. Pallavicini, J. Strähle, K. Wurst, Reactions of Zr(η^6-benzene) ($AlCl_4$)$_2$ with Alkynes: Cyclooligomerization Reactions and Crystal and Molecular Structure of the Seven-Membered Metallacycle [ZrCPh($CPh)_4$CPh][(μ-Cl)$_2AlCl_2$]$_2$, Organometallics 10 (1991) 896–901; (f) M. Martinez, M. del Carmen Michelini, I. Rivalta, N. Nino Russo, E. Sicilia, Acetylene Cyclotrimerization by Early Second-Row Transition Metals in the Gas Phase. A Theoretical Study, Inorg. Chem. 44 (2005) 9807–9816.

[10] (a) K. Yamamoto, H. Nagae, H. Tsurugi, K. Mashima, Mechanistic understanding of alkyne cyclotrimerization on mononuclear and dinuclear scaffolds: [4 + 2] cycloaddition of the third alkyne onto metallacyclopentadienes and dimetallacyclopentadienes, 45, Dalton Trans, 2016, pp. 17072–17081; (b) K. Yamamoto, H. Tsurug, K. Mashima, Direct Evidence for a [4+2] Cycloaddition Mechanism of Alkynes to Tantallacyclopentadiene on Dinuclear Tantalum Complexes as a Model of Alkyne Cyclotrimerization, 2015 Chem. – Eur. J, 21 11369–11377.

[11] (a) C. Bianchini, K.G. Caulton, C. Chardon, M.-L. Doublet, O. Eisenstein, S.A. Jackson, T.J. Johnson, A. Meli, M. Peruzzini, W.E. Streib, A. Vacca, F. Vizza, Mechanism of Acetylene Cyclotrimerization Catalyzed by the *fac*-IrP_3^+ Fragment: Relationship between Fluxionality and Catalysis, Organometallics 13 (1994) 2010–2023; (b) I. Kabdas, A. Keles, T. Olmez-Hanci, O. Tunay, I. Arslan-Alaton, Treatment of phthalic acid esters by electrocoagulation with stainless steel electrodes using dimethyl phthalate as a model compound, J. Hazard. Mater. 171 (2009) 932–940.

[12] APEX3 Version5-0 and SAINT Version 8.37A, Bruker AXS, Inc, Madison, WI, USA, 2016.

[13] SADABS Version 2016/2 L. Krause, R. Herbst-Irmer, G.M. Sheldrick, D. Stalke, J. Appl. Cryst 48 (2015) 3–10.

[14] (a) G.M. Sheldrick, SHELXT, Acta Cryst 71 (2015) 3–8 A; (b) G.M. Sheldrick, SHELXL, Acta Cryst 71 (2015) 3–8 C.

[15] O.V. Dolomanov, L.J. Bourhis, T.J. Gildea, J.A.K. Howard, H. Puschmann, OLEX2: a complete structure solution, refinement and analysis program, J. Appl. Cryst 42 (2009) 339–341.

[16] D.H. Farrar, P.F. Jackson, B.F.G. Johnson, J. Lewis, J.N. Nichol, A High-yield Synthesis of $Ru_5C(CO)_{15}$ by the Carbonylation of $Ru_6C(CO)_{17}$; the X-Ray Structure Analyses of $Ru_5C(CO)_{15}$ and $Ru_5C(CO)_{14}PPh_3$, J. Chem. Soc., Chem. Comm. (1981) 415–416.

[17] D.M.P. Mingos, Polyhedral Skeletal Electron Pair Approach, Acc. Chem. Res 17 (1984) 311–319.

[18] (a) P.J. Dyson, B.F.G. Johnson, J. Lewis, M. Martinelli, D. Braga, F. Grepioni, Stepwise Formation of the Bis(benzene)hexaruthenium Carbido Carbonyl Cluster $Ru_6C(CO)_{11}$(η^6-C_6H_6)(μ_3-η^2:η^2:η^2-C_6H_6) from $Ru_6C(CO)_{17}$, J. Am. Chem. Soc 115 (1993) 9062–9068; (b) P.J. Bailey, D. Braga, P.J. Dyson, F. Grepioni, B.F.G. Johnson, J. Lewis, P. Sabatino, The Synthesis, Molecular Structure and Interconversion of Two Novel Benzene-coordinated Pentaruthenium-Carbido Cluster Isomers [$Ru_5C(CO)_{12}$(μ_3-η^2:η^2:η^2-C_6H_6)] and [$Ru_5C(CO)_{12}$(η^6-C_6H_6)], J . Chem. Soc., Chem. Commun. (1992) 177–178.

[19] (a) G. Gervasio, E. Sappa, L. Marko, Synthesis and crystal structure of [Co2(CO)4(PhC≡CC(O)CH3)3]. Its role in the cyclotrimerization of 1-phenylbut-1-yn-3-one to 1,3,5-triphenyltris(carboxymethyl) benzene, *J. Organomet. Chem.* 444 (1993) 203–209.; (b) R.S. Dickson, P.J. Fraser, B.M. Gatehouse, Crystal and Molecular Structure of a Racemic Complex: η-[1-3,6-η:1,4-6 η-1,3,6-tris(trifluoromethyl)hexa-1,3,5-trien-l,6-diyl]-bis (dicarbonylcobalt)(Co-Co), J. Chem. Soc., Dalton Trans (1972) 2278–2282; (c) G. Wilke, H. Benn, R. Goddard, C. Krüger, B. Pfeil, Intermediates of the cyclotrimerization of 2-butyne with a chromium catalyst, Inorg. Chim. Acta 198-200 (1992) 741–748; (d) M. Green, P.A. Kale, R.J. Mercer, Pathways for Carbon-Chain Growth Reactions at a Dimolybdenum Centre, J. Chem. Soc, Chem. Commun. (1987) 375–377; (e) S.A.R. Knox, R.F.D. Stansfield, F.G.A. Stone, M.J. Winter, P. Woodward, The Sequential Linking of Alkynes at Dichromium and Dimolybdenum Centres; X-Ray Crystal Structure of [$Cr_2(CO)$(μ-C_4Ph_4)(μ-C_5H_5), J. Chem. Soc., Dalton Trans (1982) 173–185.

[20] B.F.G. Johnson, J. Lewis, S.W. Sankey, K. Wong, M. McPartlin, W.J.H. Nelson, An Improved Synthesis of the hexaruthenium carbido Cluster $Ru_6(C)(CO)_{17}$. X-ray structure of the Salt [$Ph_4As]_2$[$Ru_6(C)(CO)_{16}$], J. Organomet. Chem. 191 (1980) C3–C7.